Available online at www.sciencedirect.com

SciVerse ScienceDirect

Procedia Engineering 57 (2013) 456 – 465

Procedia Engineering

www.elsevier.com/locate/procedia

11th International Conference on Modern Building Materials, Structures and Techniques, MBMST 2013

Investigation and Modelling of the Impact of Reinforcement Diameter in Concrete on Shapes of Impedance Spectra

Mariusz Jaśniok*

Department of Building Structures, Silesian University of Technology, Akademicka str. 5, 44-100 Gliwice, Poland

Abstract

The impedance test results of the steel reinforcement of various diameters, which was passivated and corroded in concrete specimens, were analysed. The impedance plots clearly indicated the tendencies for spectra shapes of steel rebars to change depending on their diameters. A 3-dimensional model of steel-concrete system was developed to explain the observed effect. This system was composed of the identical electrical equivalent circuits connected in parallel. Each equivalent scheme was characteristic for a theoretical conductive path during the measurement, which was defined between a counter-electrode and the reinforcement. This model was used with the rectangular counter electrode to simulate the formation of impedance spectra characteristic for a single reinforcing bar with the concrete cover of any thickness, a variable diameter and a variable polarization area. The simulation modelling the impact of various reinforcement diameters verified the tendencies for impedance spectra of steel in concrete to change their shapes. The improved of fitting quality of the model spectra to the experimental ones were obtained by considering in that model the moisture content in concrete.

Keywords: reinforced concrete; reinforcing steel; corrosion; EIS; electrochemical impedance plots; investigation; model.

Introduction

The corrosive degradation of reinforced concrete structures [1-3] presents a real threat to their safe use and the reliability [4], [5]. Thus, the competence for assessing the corrosion risk properly and taking proper repair actions if necessary, is extremely important [6-10]. The application of the polarization techniques [11] and particularly the method of impedance spectroscopy for assessing the corrosion rate of the reinforcement in the reinforced concrete structures encounters considerable difficulties [12]. These problems are related to complex measurement conditions and the complicated testing system. The studies are carried out using the potentiostat in a three-electrode system, in which the structure reinforcement (made of long steel bars) serves as the working electrode, and the electrode of known and satisfactory reversible potential serves as the reference electrode. The counter-electrode is applied to the surface of the reinforced concrete element to make the reinforcement polarization possible. The counter-electrode along with the reference electrode in a single enclosure formed the so called measuring head. The use of the head created a situation considerably different from the laboratory conditions form the measurement in an electrochemical vessel in which the large counter electrode uniformly polarizes the small tested electrode of a simple geometry. Regarding the measurements on the reinforcement in the reinforced concrete elements, the area of the tested electrode was significantly larger than that of the counter electrode applied to concrete. This resulted in the very non-uniform polarization of steel rebars. Moreover, the polarization area of the reinforcement required for assessing the rate of the electrochemical processes was unknown. The additional counter electrode in a form of a guard ring reducing the distribution of the polarization currents solves the above problem in large – *cf* [13]. The additional setback to interpret correctly the measurements on steel impedance in concrete were caused by various activity levels of the reinforcement insert surfaces.

* Corresponding author.
E-mail address: mariusz.jasniok@polsl.pl

doi:10.1016/j.proeng.2013.04.059

The first attempt to apply the impedance spectroscopy for monitoring the corrosion of concrete specimens immersed in salt water was described in the paper [14]. The authors suggested that the electrical equivalent circuit composed of two *R-C* systems in series, one of them with Warburg impedance, could be used to analyse the obtained impedance spectra. In consecutive years, other papers describing new proposals of equivalent schemes were published. However, the studies were mainly carried out on small specimens. A different interpretation of the impedance spectrum for the concrete reinforcement was proposed in the paper [15] describing the electrical model of steel-concrete system based on the transmission line. This paper described an interesting, but not experimentally verified, method of detecting local corrosion on long reinforcement rods. The paper [16] presented a slightly different approach towards modelling the response to the AC polarization of long rebars in concrete. Similarly to the model of transmission lines, the authors connected a few Randles circuits in parallel, each of them was assigned to a conceptually selected section of the long reinforcement rods with the cover. Additionally, the reference electrode and the counter electrode were assumed to be geometrically concentrated at one point. The above briefly described evolution of modelling the system of the long reinforcement bars in concrete demonstrated that the traditional modelling of single electrical equivalent schemes did not allow the electrochemistry of the tested system to be fully represented.

The study on the above papers and the own studies on corrosion performed on the large-sized reinforced concrete structures became a source of inspiration for making an attempt to prepare the model description of the impact of the complex steel-concrete system geometry on the shapes of obtained impedance spectra. The experimental tests and the model simulations described in this paper refer to the system composed of a long reinforcing bar placed in a cuboidal concrete specimen.

1. Course and results of experimental studies

5 types of specimens having identical overall dimensions of 250×100×100 mm were developed for the experimental purpose – Fig. 1a. The elements were made in two runs *S1* and *S2* – 10 pieces in total. The series *S1* was made of concrete characterized by the best protective properties regarding reinforcing steel, while the series *S2* was made of concrete with reduced protective properties regarding steel, because 2% $CaCl_2$ related to cement mass was added to the concrete mix.

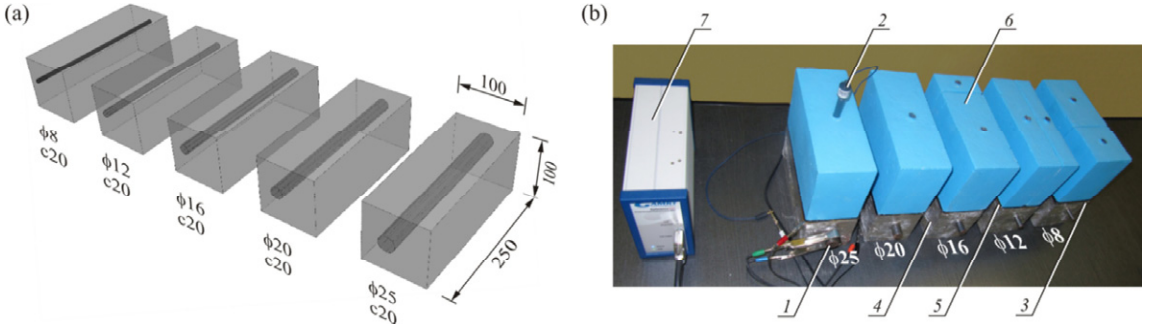

Fig. 1. Specimens (a) and the test stand (b) for measuring impedance of reinforcing steel in concrete – described in the text.

The rebars of five diameters, ϕ = 8, 12, 16, 20 and 25 mm respectively, were used while maintaining the constant cover thickness c = 20 mm. Each concrete specimen was reinforced with a single rebar made of smooth steel of S235JR grade. The concrete mix, with water-cement ratio w/c = 0.43, per 1 m^3 of concrete was composed of: 489 kg of Portland cement 32.5R; 501 kg of fine aggregate with the fraction up to 2 mm; 1168 kg of coarse aggregate with the fraction of 2-8 mm and 212 litres of water.

The impedance was measured in a three-electrode system at a test stand illustrated in Fig. 1b. The rebars of various diameters and the same length of 250 mm were used as the working electrodes *1*. The electrode Cl^-/AgCl,Ag in the plastic enclosure served as the reference electrode *2*. And a sheet of stainless steel of 250×100 m dimensions and 2 mm width was used as the counter electrode *3*. A hole of 7 mm diameter was made in the geometric centre of gravity in the counter electrode *3* to introduce a glass end of the reference electrode *2*. The specimens and the counter electrodes were protected with a foil *4* to minimize the impact of changes in concrete moisture during the measurements. The counter electrodes *3* were placed on the top surface of the specimen using wet felt *5* to ensure the proper electric contact of the counter electrode and the reference electrode with concrete. The counter electrode's uniform contact with concrete through the felt was obtained by concrete weights *6* which provided the optimum pressure of 30 g/cm^2. The described three-electrode system was connected to the potentiostat *7* which controlled the performance of impedance measurements.

24 hours before the impedance measurements, the specimens were immersed in tap water up to the half of the reinforcement cover thickness to activate the electrode processes. The wet surface of the specimen was dried with absorbent paper directly after taking it out of water, and the moisture content in ca. 50 mm concrete layer towards the cover thickness was measured in 9 uniformly arranged spots using the dielectric hygrometer.

The main impedance measurements were performed with *Gamry Reference 600* potentiostat after ca. 2-3 hours of potential stabilization of the reinforcement. The measurements were conducted in a potentiostatic mode at the fixed range of frequencies 1 MHz÷10 MHz and the potential amplitude of 10 mV regarding the stationary potential of the reinforcement.

Fig. 2 illustrates a 3D view of the shapes of impedance spectra for five steel rebars of ϕ8, ϕ12, ϕ16, ϕ20 and ϕ25 mm diameters in the concrete specimens of *S1* and *S2* series. Additionally, a classic presentation of the same measurement results was shown on the Nyquist (Fig. 5c, h) and Bode plots (Fig. 5e, j) in the chapter on the comparative analysis of the studies using the theoretical model.

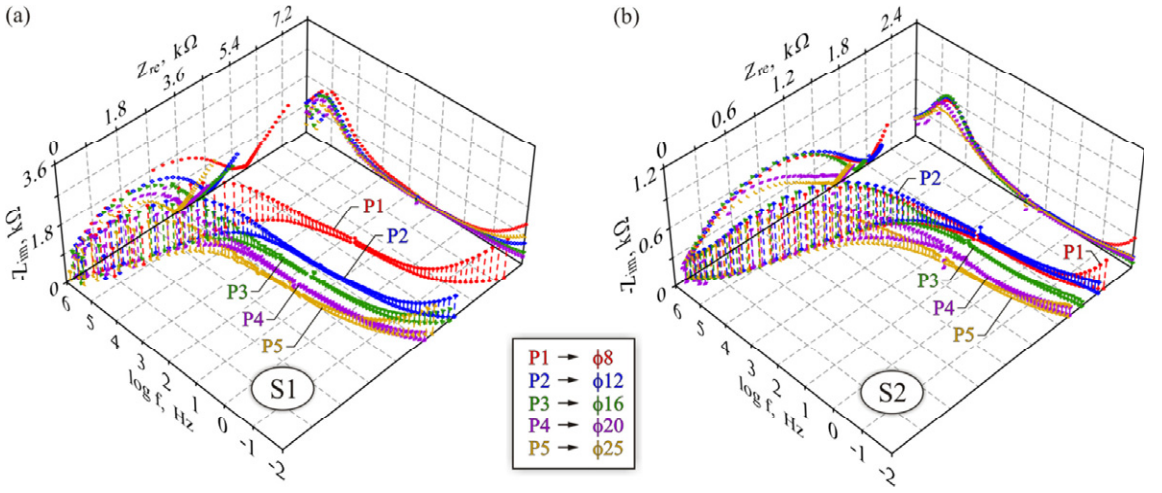

Fig. 2. The results of impedance measurements on steel rebars of ϕ = 8, 12, 16, 20 and 25 mm diameters in the concrete specimens of *S1* and *S2* series.

The comparison of these two groups of spectra (Fig. 2a, b) indicated that for concrete of *S1* series, the impedance of the steel-concrete system was over three times lower than in the case of concrete of *S1* series. This effect is more visible on the Bode plots (Figs 5e, 5j), at which the impedance modulus *Z* of reinforcing steel in *S1* concrete at low frequencies reached the level of 4.3÷7.8 kΩ, whereas *S2* concrete reached the level of 1.8÷2.4 kΩ. The phase shift angles at low-frequencies characterizing the properties of steel in *S2* concrete, were nearly three times lower than in *S1* concrete, Fig. 5e, j. Moreover, a slope and a distribution length of the real impedance intercepts on the complex plane Z_{re}–Z_{im} (Fig. 5c, h and Fig. 2) in *S2* concrete were shorter than on the plots for *S1* series. The presented differences between these two groups of spectra can support the initial assumption about the depassivation of steel in *S2* concrete containing chlorides and the passivation of steel in *S1* concrete.

Besides the above discussed features describing the electrochemical state of steel in concrete, a very clear tendency towards changes in spectra shapes resulting from various geometries of the tested steel-concrete systems were observed on the impedance plots. A very clear relationship could be observed which demonstrated that the spectra were getting smaller and at the same time shifted towards lower values of the real impedance axis along with the increasing diameter of the tested rebars, see Figs 2, 5c, h. The highest impedance values were obtained for steel of ϕ8 mm diameter in *S1* concrete (*P1* spectrum), whereas the lowest values were obtained for steel of ϕ25 mm diameter in *S2* concrete (*P5* spectrum). The model described below was used to make an attempt to explain theoretically the effects related to the impact of the geometry of the steel-concrete system on the shapes of obtained spectra.

2. The "3D" model of the steel-concrete system

The three-electrode measurement system to analyse and simulate the measurements of reinforcing steel impedance in concrete were subjected to modelling. The 3D visualisation of the system is presented in Fig. 3.

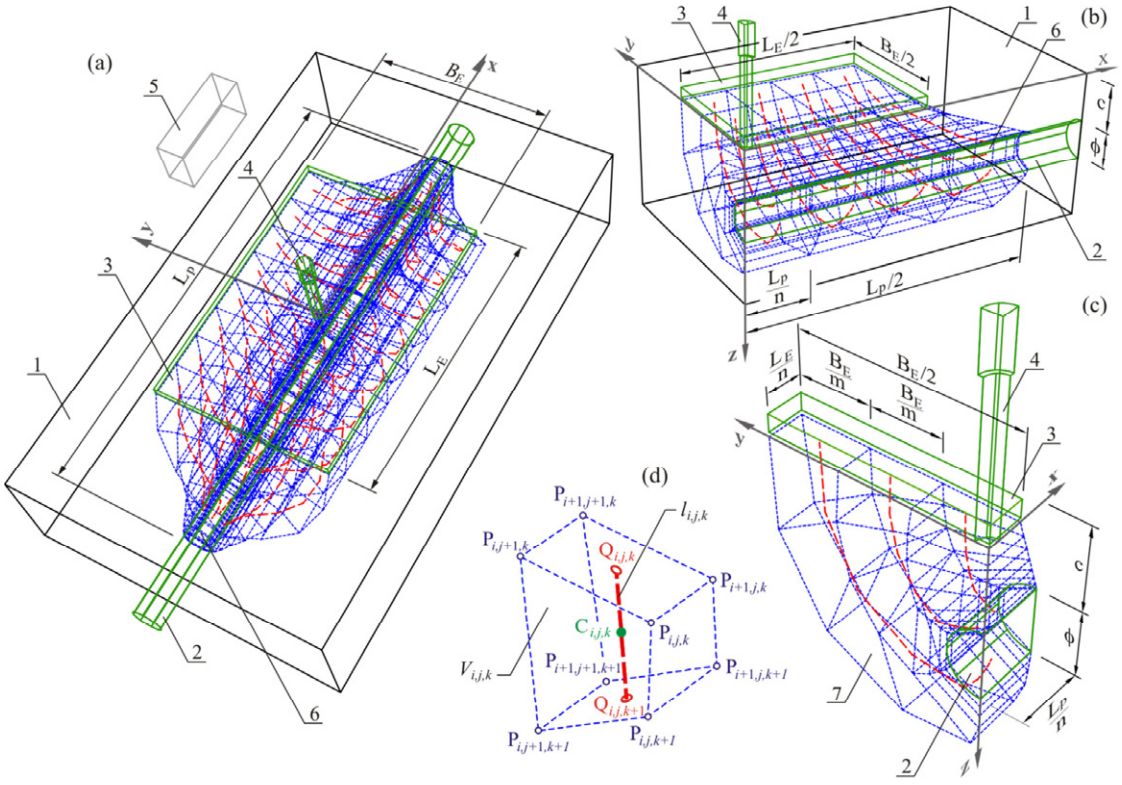

Fig. 3. Assumptions for the '3D' model of the steel–concrete system to simulate and analyse the impedance tests: (a) a whole system, (b) a quarter of system with two symmetry planes, (c) a strip of system with three theoretical conductive paths, (d) a solid concrete element – described in the text.

Considering the typical three-electrode system used in electrochemistry to measurements the polarization of metals in electrolytes, concrete in the shape of solid with at least one plane surface *1* was the electrically conducting medium in the modelling system during the measurements. The steel rebar *2* of ϕ diameter and *L* length, whose shortest distance from the concrete flat surface, namely, the cover thickness was *c*, served as the working electrode. The metal counter electrode *3* in the rectangular shape of $L_E \times B_E$ dimensions was put on the concrete flat surface to place the edge L_E parallel to the axis of the reinforcement bar and the edge B_E symmetrically to the geometric centre of the rebar cross-section. The reference electrode *4* of constant and known potential was applied to the concrete surface through the hole in the geometric centre of the rectangular contour of the counter electrode *3*. All three electrodes were connected to the potentiostat *5* which controlled the performance of an impedance measurement. The reinforcement surface *6* in the shape of the cylinder side surface of the height L_p and the base circumference $B_p = \pi\phi$, situated symmetrically to the geometric centre of the counter electrode *3* was assumed to be polarized during the measurement.

The Cartesian spatial system of coordinates was introduced into the model and the centre of the system was established on the concrete flat surface *1* inside the electrode *4*. The *x* axis of the coordinate system was parallel to the rebar *2* axis, and the *y* axis was parallel to the edge B_E of the counter electrode *3*, while the *z* axis coincided with the longitudinal axis of the reference electrode *4*. Regarding the described assumptions, the modelling system has two symmetry planes *x*-*z* and *y*-*z*.

During the impedance measurement, the theoretical conductive paths were defined in the modelling three-electrode measurement system. It was assumed that the theoretical conductive paths *7* (Fig. 3c) were the elongated curvilinear concrete solids whose top surface was on the counter electrode surface *3*, and the bottom surface was on the surface of the working electrode *2*. The model was divided into *n* elements towards the *x* axis, *m* elements towards the *y* axis and *p* elements towards the *z* axis (*n*, *m* – even numbers) to determine the theoretical conductive paths. Consequently, both the counter electrode and the working electrode were composed of the same number $n \times m$ of surface elements since their thickness was not important for the course of the described physical and chemical effect. However, concrete present between these electrodes, serving as the electrically conducting medium was divided into irregular octagonal solid elements $n \times m \times p$ in number. The assumed division into the surface and solid elements was the basis for defining the geometrical relationships to determine the coordinates creating the spatial grid of the model nodes.

The definitions of local and global geometric factors for steel and concrete were introduced for the purpose of considering the measurement system in the model of complex geometry.

The local geometric factor for concrete $\gamma^{c}_{i,j}$ on the theoretical conductive path $T_{i,j}$ was defined as the sum of length quotients of the current line segments $l_{i,j,k}$ to the conventional surface of the current flow $S_{i,j,k}$ through the solid elements of $V_{i,j,k}$ volume (Fig. 3d). The factor $\gamma^{c}_{i,j}$ was calculated from the following relationship:

$$\gamma^{c}_{i,j} = \sum_{k=1}^{p} \frac{l_{i,j,k}}{S_{i,j,k}}, \qquad S_{i,j,k} = \psi_{i,j,k} \frac{V_{i,j,k}}{l_{i,j,k}}, \qquad k = 1, 2, .., p\,. \tag{1}$$

And the factor $\psi_{i,j,k}$ in the formula (1) was determined from the following relationship:

$$\psi_{i,j,k} = \frac{V^{w}_{i,j,k}}{V_{i,j,k}} = \frac{m^{w}_{i,j,k}}{m^{c}_{i,j,k}} \frac{\rho^{c}}{1} = w_{i,j,k}\ \rho^{c}\,, \tag{2}$$

where $V^{w}_{i,j,k}$ is water volume in the volume $V_{i,j,k}$ of the solid element. The volume of water is expressed as the quotient of water mass $m^{w}_{i,j,k}$ in the volume $V_{i,j,k}$ and its bulk density $\rho^{w}_{i,j,k}$, and similarly, the volume of the solid element is expressed as the quotient of the dry concrete mass in the volume $V_{i,j,k}$ and its bulk density $\rho^{c}_{i,j,k}$. Then, assuming that the bulk density of concrete was the same in each solid element $\rho^{c}_{i,j,k} = \rho^{c}$ and the bulk density of water in each solid element was the same and equal to unity $\rho^{w}_{i,j,k} = \rho^{w} = 1.0$ g/cm^3. The factor $\psi_{i,j,k}$ subjected to basic conversions can be expressed as the product of concrete mass moisture $w_{i,j,k}$ in the element of volume $V_{i,j,k}$ and mean bulk density of concrete ρ^{c} – *cf.* the formula (2).

The local geometric factor for steel $\gamma^{s}_{i,j}$ was defined as the converse product of the rebar polarization area $A^{p}_{i,j}$ (located at the end of the theoretical conductive path $T_{i,j}$) and the quotient of the current line length $l_{i,j}$ to the average length of current line l_{mid}. The factor $\gamma^{s}_{i,j}$ was calculated from the expression:

$$\gamma^{s}_{i,j} = \frac{1}{A^{p}_{i,j}} \cdot \frac{l_{i,j}}{l_{mid}}, \qquad l_{i,j} = \sum_{k=1}^{p} l_{i,j,k}\,, \quad i = 1, 2, .., \frac{n}{2}, \quad j = 1, 2, .., \frac{m}{2}, \qquad l_{mid} = \frac{1}{\frac{n}{2} \cdot \frac{m}{2}} \sum_{i=1}^{\frac{n}{2}} \sum_{j=1}^{\frac{m}{2}} l_{i,j}\,. \tag{3}$$

The formulas describing the global geometric factors for the modelling system were derived from the local geometric factors for concrete $\gamma^{c}_{i,j}$ and steel $\gamma^{s}_{i,j}$ characterizing the theoretical conductive path $T_{i,j}$ defined by the formulas (1) and (2). Regarding two planes of the model symmetry, the global geometric factor for concrete geometry γ^{c} and for steel geometry γ^{s} were defined as:

$$\gamma^{c} = \frac{1}{\sum_{i=1}^{\frac{n}{2}} \sum_{j=1}^{\frac{m}{2}} \frac{4}{\gamma^{c}_{i,j}}}, \qquad \gamma^{s} = \frac{1}{\sum_{i=1}^{\frac{n}{2}} \sum_{j=1}^{\frac{m}{2}} \frac{4}{\gamma^{s}_{i,j}}}. \tag{4}$$

The factor γ^{c} describes the volume of concrete through which AC current flows between the counter electrode and the rebar during the impedance measurements. It can be observed that, for a specific case, if the length $l_{i,j}$ of all current lines corresponded to the length of the averaged line l_{mid}, then the inverse of a value of the total polarization area A^{p} of the rebar defined as below would be assigned to the factor γ^{s}

$$A^{p} = 4 \cdot \sum_{i=1}^{\frac{n}{2}} \sum_{j=1}^{\frac{m}{2}} A^{p}_{i,j}\,. \tag{5}$$

Each theoretical conductive path $T_{i,j}$ was assumed to be described by the impedance $Z^{c}_{i,j}$, characterizing concrete of $\gamma^{c}_{i,j}$ geometric factor, which was combined in series with the impedance $Z^{s}_{i,j}$ characterizing steel of $\gamma^{s}_{i,j}$ geometric factor. For analysing the impedance spectra, an adequately selected combination of resistances $R_{i,j}$ and constant phase elements (*CPE*) described by the parameters $Y_{i,j}$ and $\alpha_{i,j}$ [17] was usually sufficient to characterize the electrochemical properties of concrete

and steel using the electrical equivalent circuit. Thus, it can be generally assumed that the following function describes the equivalent impedance $Z^s_{i,j}$ of steel at the end of the theoretical conductive path :

$$Z^s_{i,j} = Z^s_{i,j}(R^s_{i,j}, Y^s_{i,j}, \alpha^s_{i,j}), \qquad R^s_{i,j} = R^s \cdot \gamma^s_{i,j}, \quad Y^s_{i,j} = Y^s \cdot \frac{1}{\gamma^s_{i,j}}, \quad \alpha^s_{i,j} = \alpha^s. \tag{6}$$

On the other hand, the equivalent impedance $Z^c_{i,j}$ of concrete along the theoretical conductive path is described by the similar function:

$$Z^c_{i,j} = Z^c_{i,j}\left(R^c_{i,j}, Y^c_{i,j}, \alpha^c_{i,j}\right), \qquad R^c_{i,j} = R^c \cdot \gamma^c_{i,j}, \quad Y^c_{i,j} = Y^c \cdot \frac{1}{\gamma^c_{i,j}}, \quad \alpha^c_{i,j} = \alpha^c. \tag{7}$$

The parameters R^s and Y^s in the relationship (6) characterize the electrochemical properties with reference to the unit area of reinforcing steel, while the analogical parameters R^c and Y^c in the equation (7) describe the electrochemical properties with reference to the unit volume of concrete. The parameters α^s i α^c are the dimensionless coefficients. The above relationships can be used to introduce the term of the elementary electrical equivalent circuit. It is an electrical scheme, identical at every theoretical conductive path $T_{i,j}$, composed of suitably selected combination of resistances and constant phase elements, whose parameters $R_{i,j}$, $Y_{i,j}$, $\alpha_{i,j}$ were calculated considering the geometric factors for concrete $\gamma^c_{i,j}$ and steel $\gamma^s_{i,j}$. The exemplary elementary electrical equivalent circuit is shown in Fig. 4b. Regarding the two planes of symmetry, the final total equivalent impedance of the modelling steel-concrete system can be determined from the following expression:

$$Z = \frac{1}{\sum_{i=1}^{\frac{n}{2}} \sum_{j=1}^{\frac{m}{2}} \left(\frac{4}{Z^c_{i,j} + Z^s_{i,j}} \right)}. \tag{8}$$

3. The analysis of studies according to the '3D' model

The analysis of the spectra from both 5-element series *S1* and *S2* according to the model '3D' began from the stage, at which the so called initial spectrum – obtained at the known length of the polarization range L_p, was established. In the discussed tests, all the steel-concrete systems provided the polarization of the whole reinforcement area, namely, the range L_p was known and corresponded to the length L of the rebar – *cf.* Fig. 3a. So, we were able to select the initial spectrum in an optional way. Both selected initial spectra (marked as *P1* in Fig. 2 and Fig. 5) were analysed in an conventional way using the adequately selected equivalent electrical circuit [17] shown in Fig. 4a.

In the diagram shown in Fig. 4a, R^1 denotes the resistance of liquid phase, while R^2, R^{2a} denote the resistance of a double layer at the interface of liquid and solid phases of concrete, which capacity is described by Y^2, α^2, Y^{2a}, α^{2a} parameters of the *CPE*. The electrochemical parameters of the transient layer of steel – concrete are described by the *CPE* having the parameters Y^3, α^3, while the double layer at the interface of pore solution and reinforcing steel is described by the *CPE* having the parameters Y^0, α^0 with the charge transfer resistance R^t connected in parallel – *cf* [18].

The method of iterative fitting was used to determine the electrochemical characteristics of concrete and steel specified in that scheme (Fig. 4a), namely, the resistances r^1, r^2, r^{2a}, r^t and the parameters of constant phase elements y^2, α^2, y^{2a}, α^{2a}, y^3, α^3, y^0, α^0. The numerical values of the specified parameters and the statistical evaluation of fitting quality of *S1* and *S2* spectra are listed in Table 1.

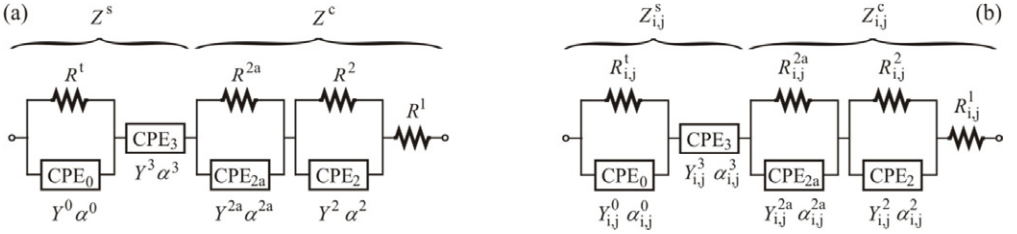

Fig. 4. Circuits used to analyse the impedance spectra of steel in concrete: (a) equivalent electrical circuit, (b) elementary equivalent electrical circuit.

Table 1. Electrochemical parameters and the evaluation of fitting quality of initial spectra of steel in *S1* and *S2* concrete calculated according to the relationships given in Table 2

Parameters of initial spectra with no reference to the material area or volume				Unit parameters							
				common for 5 spectra of *S1* and *S2* series, calculated acc. to '3D' model				converted only with reference to the polarization area of steel			
	S1	*S2*			*S1*	*S2*			*S1*	*S2*	
r^1 =	0	0	Ω	R^1 =	0	0	Ω·cm	$\underline{R}^1$ =	0	0	Ω·cm
r^2 =	4.543	0.639	kΩ	R^2 =	21.18	3.576	kΩ·cm	$\underline{R}^2$ =	280.6	39.47	kΩ·cm
r^{2a} =	1.154	1.293	kΩ	R^{2a} =	5.380	7.235	kΩ·cm	$\underline{R}^{2a}$ =	71.28	79.86	kΩ·cm
y^2 =	3.058	80.92	nF·s$^{\alpha-1}$	Y^2 =	0.656	14.46	nF·s$^{\alpha-1}$/cm	$\underline{Y}^2$ =	0.050	1.310	nF·s$^{\alpha-1}$/cm^2
α^2 =	0.816	0.752		α^2 =	0.816	0.752		$\underline{\alpha}^2$ =	0.816	0.752	
y^{2a} =	1775	284.0	nF·s$^{\alpha-1}$	Y^{2a} =	380.7	50.76	nF·s$^{\alpha-1}$/cm	$\underline{Y}^{2a}$ =	28.74	4.598	nF·s$^{\alpha-1}$/cm^2
α^{2a} =	0.583	0.669		α^{2a} =	0.583	0.669		$\underline{\alpha}^{2a}$ =	0.583	0.669	
y^3 =	2112	4260	μF·s$^{\alpha-1}$	Y^3 =	26.03	52.51	μF·s$^{\alpha-1}$/cm^2	$\underline{Y}^3$ =	34.19	68.97	μF·s$^{\alpha-1}$/cm^2
α^3 =	0.269	0.077		α^3 =	0.269	0.077		$\underline{\alpha}^3$ =	0.269	0.077	
y^0 =	4302	3090	μF·s$^{\alpha-1}$	Y^0 =	53.03	380.9	μF·s$^{\alpha-1}$/cm^2	$\underline{Y}^0$ =	69.65	500.3	μF·s$^{\alpha-1}$/cm^2
α^0 =	0.641	0.830		α^0 =	0.641	0.830		$\underline{\alpha}^0$ =	0.641	0.830	
r^t =	4.804	1.510	kΩ	R^t =	389.7	122.5	kΩ·cm^2	$\underline{R}^t$ =	296.7	93.26	kΩ·cm^2
a =	5	2	%	a =	5	2	%	A^p =	61.76	61.76	cm^2
χ^2 =	540.9	119.8		χ^2 =	533.4	120.6		i_{kor} =	0.18	0.54	μA/cm^2
q =	1.90	0.89		q =	1.89	0.90		CR =	0.002	0.006	mm/year

The electrochemical parameters denoted by small letters for the purpose of this analysis, indicated the characteristics with no reference to any area or volume of the material. The fitting quality of the modelling spectra to the experimental ones was assessed using the factor q [19] described by the following formula:

$$q = \sqrt{\frac{\chi^2}{2N - N_p}}, \qquad \chi^2 = \sum_{i=1}^{N}\left[\left(\frac{Z^e_{re,i} - Z^c_{re,i}}{\sigma_i}\right)^2 + \left(\frac{Z^e_{im,i} - Z^c_{im,i}}{\sigma_i}\right)^2\right]. \tag{9}$$

In the above formula, N denotes a number of frequencies, at which points of the impedance spectrum were determined, N_p denotes a number of determined variables in the model of steel – concrete system, whereas χ^2 is the objective function. The parameters $Z^e_{re,i}$ and $Z^e_{im,i}$ are the real and imaginary components respectively, of the impedance obtained during the experimental studies, while $Z^c_{re,i}$ and $Z^c_{im,i}$ are the corresponding components of the impedance calculated according to the '3D' model. The value σ_i in the expression (9) describes the standard deviation of the measurement at i-letter frequency estimated as $a \cdot |Z^e_i|$. The parameter $|Z^e_i|$ is the modulus of the impedance measured at i-letter frequency, whereas the constant a is the estimated measuring error expressed in percentage.

Then, using the geometry of the tested system modelled into the original software and using the identified elementary equivalent electric (Fig. 4b), the global geometric factors for concrete γ^c and steel γ^s geometries were calculated automatically. These factors were used to determine the unit parameters of the '3D' model denoted by capital letters R^t, Y^0, α^0, Y^3, α^3, and R^1, R^2, R^{2a}, Y^2, α^2, Y^{2a}, α^{2a}. The numerical values of these parameters are shown in Table 1. The corresponding conversion formulas are listed in Table 2.

The unit parameters of the '3D' model are to be understood as the electrochemical parameters assumed to be independent from the geometry of the tested 'reinforcement – concrete – counter electrode' system. The papers dealing with the discussed issue usually present the electrochemical parameters of concrete and steel, which are calculated with regard to the polarization area of steel [20-21], although there are some departures from that rule – *cf* [22]. However, to refer the results from the analysis obtained according to the '3D' model to the "typical" unit parameters, the simple relationships for converting all concrete and steel characteristics to the polarization area of steel are listed in Table 2. The typical unit parameters were denoted by the underlined capital letters, that is, $\underline{R}^1$, $\underline{R}^2$, $\underline{R}^{2a}$, $\underline{R}^t$ and $\underline{Y}^2$, $\underline{\alpha}^2$, $\underline{Y}^{2a}$, $\underline{\alpha}^{2a}$, $\underline{Y}^3$, $\underline{\alpha}^3$, $\underline{Y}^0$, $\underline{\alpha}^0$, and their numerical values are listed in Table 1.

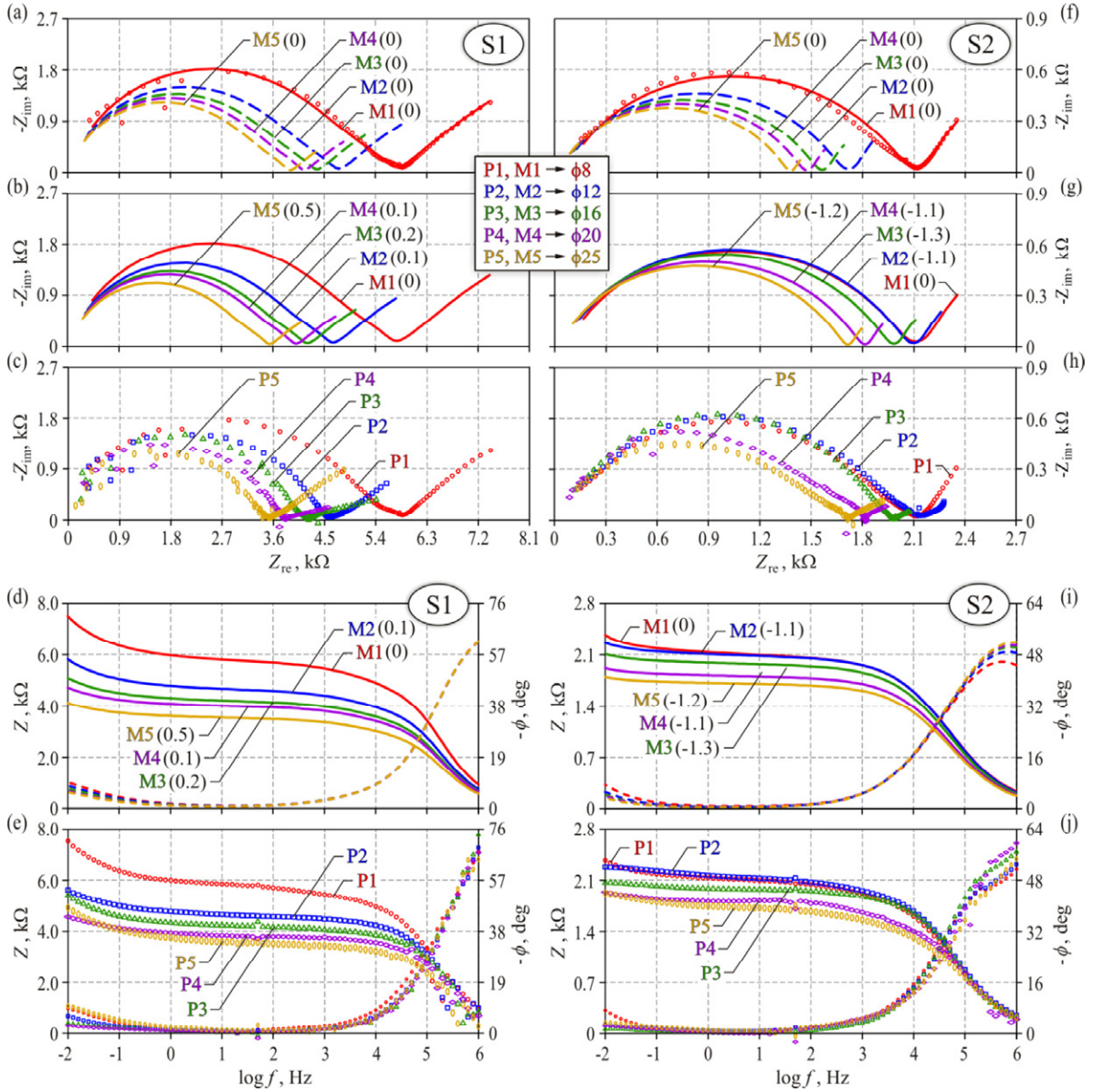

Fig. 5. The comparative analysis of test results and modelling simulations of the impact of rebar diameters on the shapes of impedance spectra of steel in concrete: (a), (f) – first stage of model simulation in Nyquist plots; (b), (g) – second (last) stage of model simulation in Nyquist plots; (c), (h) – test results in Nyquist plots; (d), (i) –last stage of model simulation in Bode plots; (e), (j) – test results in Bode plots – described in the text.

Finally, the determined unit parameters (R^1, R^2, R^{2a}, … in Table 1) of concrete and steel were used to generate the theoretical spectra *M1*, *M2*, *M3*, *M4* and *M5* (Fig. 5) according to the assumptions of the '3D' model. During the modelling simulation of spectra, only one parameter from the system geometry, namely, the reinforcement diameter was varying in order to compare the model spectra with the experimental ones *P1*, *P2*, *P3*, *P4* and *P5* obtained at various diameters of the rebars. The impact of the moisture content in concrete on the measurement results were expressed using the moisture content by mass in concrete $w_{i,j,k}$ in the Eq. (2). As there were no technical opportunities for measuring the spatial distribution of moisture content in concrete, the simplifying assumption was made by approximating the spot moisture by the averaged moisture content, that is, $w_{i,j,k} = w_{mid}$. For that purpose, directly before measuring the impedance, the moisture content in concrete was measured with dielectric method and conversed into the moisture content by mass according to the empirical formulas, and the arithmetic mean was assumed to be $w_{mid.}$ The conversion formulas were obtained on the basis of

the correlation tests on the independent concrete specimens formed simultaneously with the basic elements. The same elements were used to determine the bulk density of concrete ρ^c, which term appears in the Eq. (2).

Table 2. The relationships between the electrochemical parameters considered in the analysis of impedance spectra of steel in concrete according to the '3D' model

STEEL			CONCRETE		
Parameters with no reference to the material area or volume	Unit parameters		Parameters with no reference to the material area or volume	Unit parameters	
	calculated acc. to '3D' model	converted with reference to the polarization area of steel		calculated acc. to '3D' model	converted with reference to the polarization area of steel
r^1	$R^1 = \frac{r^1}{\gamma^s}$	$\underline{R}^1 = R^1\gamma^s A^p = r^1 A^p$	r^2	$R^2 = \frac{r^2}{\gamma^c}$	$\underline{R}^2 = R^2\gamma^c A^p = r^2 A^p$
[Ω]	[Ω·cm^2]	[Ω·cm^2]	[Ω]	[Ω·cm]	[Ω·cm^2]
y^0	$Y^0 = y^0\gamma^s$	$\underline{Y}^0 = \frac{Y^0}{\gamma^s A^p} = \frac{y^0}{A^p}$	y^2	$Y^2 = y^2\gamma^c$	$\underline{Y}^2 = \frac{Y^2}{\gamma^c A^p} = \frac{y^2}{A^p}$
[F·s$^{\alpha-1}$]	[F·s$^{\alpha-1}$/cm^2]	[F·s$^{\alpha-1}$/cm^2]	[F·s$^{\alpha-1}$]	[F·s$^{\alpha-1}$/cm]	[F·s$^{\alpha-1}$/cm^2]
y^3 converted in an analogous way to y^0, α^0 and α^3 without conversion			r^1 converted in an analogous way to r^2 y^{2a} converted in an analogous way to y^2; α^2 and α^{2a} without conversion		

4. Conclusions

Fig. 5 illustrates the Nyquist and Bode plots showing the results of tests and simulations of a single diameter rebar on the shapes of impedance spectra of steel in *S1* and *S2* concrete according to the '3D' model. The experimental and theoretical spectra were not deliberately shown on the same plots because each impedance measurement was performed on an independent specimen. Thus, in spite of the fact that the identical curing conditions for concrete were provided, the electrochemical conditions of reinforcing steel and the electrical properties of concrete will never be the same, although similar.

According to the legend shown in Fig. 5, the experimental spectra were denoted by the letter *P* and the numbers from 1 to 5 corresponding to the rebar diameters of ϕ8, ϕ12, ϕ16, ϕ20 and ϕ25 mm. The modelling spectra were denoted in a similar way, however the letter *P* was replaced with the letter *M* and additionally, the increase Δw_{mid} in average moisture content by mass in concrete was shown in brackets. Δw_{mid} was defined as the difference between the measured average moisture content in concrete surrounding the rebar ϕ8 mm characterized by the initial spectrum *P1*, and the iterative fitted theoretical moisture content in concrete surrounding the remaining rebar diameters were characterized by spectra *P2*, *P3*, *P4* and *P5*. The theoretical moisture content in concrete is the moisture content by mass, at which the fitting of the modelling spectrum to the experimental one provides the best results.

On the Nyquist plot (Fig. 5a, f), a dotted line indicates the model spectra *M2*, *M3*, *M4* and *M5* obtained at the same moisture content by mass in concrete as the initial spectrum *M1*, whereas on the Nyquist (Fig. 5b, g) and Bode (Fig. 5d, i) plots, the solid line indicates the model spectra *M2*, *M3*, *M4* and *M5* after determining the theoretical moisture content in concrete. The increase in moisture content Δw_{mid} in the concrete specimens of *S1* series was observed to be very low within the range of 0.1÷0.2%, whereas in the concrete specimens of *S2* series, the increase was found within a wider range varying from –1.1 to –1.3%. The determined theoretical moisture contents approximately correspond to the measured average moisture contents by mass in the particular specimens. However, these values cannot be compared as spatial distribution of moisture content is an important issue, and not the average value.

The discussed results obtained from the impedance tests on the steel rebars of different diameters in the concrete specimens indicate a clear dependence on the various geometry of the steel – concrete system. The proposed '3D' model correctly reflects the tendencies towards changing the shapes of impedance spectra observed in the experimental studies. The improved conformity of fitting of the model spectra to the experimental ones were obtained by considering in that model the moisture content by mass in concrete, however the verification of the moisture content impact on the analysis results was of theoretical nature.

Acknowledgements

This work was performed under the research project POIG.01.01.02-10-106/09-03 “Innovative means and effective methods of improving safety and durability of structures and transport infrastructure in a strategy of sustainable development.”

References

[1] Czarnecki, L., Woyciechowski, P., 2012. Concrete Carbonation as a Limited Process and Its Relevance to Concrete Cover Thickness, ACI Materials Journal 109(3), pp. 275-282.
[2] Blaszczynski, T., 2011. The Influence of Crude Oil Products on RC Structure Destruction, Journal of Civil Engineering and Management 17(1), pp. 146-156. http://dx.doi.org/10.3846/13923730.2011.561522
[3] Klakočar-Ciepacz, M., Falewicz, P., Kuczkowska, S., Zybura, A., 2011. Modelling of corrosion of reinforcement in contact with cracked concrete cover, Corrosion Engineering, Science & Technology 46(4), pp. 353-359. http://dx.doi.org/10.1179/147842209X12559428167760
[4] Ferreira, R. M., 2010. Implications on RC Structure Performance of Model Parameter Sensitivity: Effect of Chlorides, Journal of Civil Engineering and Management 16(4), pp. 561-566. http://dx.doi.org/10.3846/jcem.2010.62
[5] Medeliene, V., Ziogas, V. A., 2010. Making Solutions for Choosing Industrial Concrete Floors and Expedience of Reliability Evaluation, Journal of Civil Engineering and Management 16(3), pp. 320-331. http://dx.doi.org/10.3846/jcem.2010.37
[6] Ali, A., Zybura, A., 2008. Application of termomechanics equations in describing chloride extraction from concrete, Transport in Porous Media 72, pp. 139-156. http://dx.doi.org/10.1007/s11242-007-9138-z
[7] Jaśniok, M., Zybura, A., 2009: Modelling the Carbonated Concrete Realkalization, Journal of Civil Engineering and Management 15(2), pp. 159-168. http://dx.doi.org/10.3846/1392-3730.2009.15.159-168
[8] Czarnecki, L., Lukowski, P., 2010. Polymer-cement concretes, Cement Wapno Beton 15(5), pp. 243-258.
[9] Kamaitis, Z., 2009. Modelling of Corrosion Protection as Standby System for Coated Reinforced Concrete Structures, Journal of Civil Engineering and Management 15(4), pp. 387-394. http://dx.doi.org/10.3846/1392-3730.2009.15.387-394
[10] Martinez, I., Andrade, C., Castellote, M., de Viedma, P.G., 2009. Advancements in non-destructive control of efficiency of electrochemical repair techniques, Corrosion Engineering Science and Technology 44(2), pp. 108-118. http://dx.doi.org/10.1179/174327808X286266
[11] Martinez, I., Andrade, C., 2011. Polarization resistance measurements of bars embedded in concrete with different chloride concentrations: EIS and DC comparison, Materials and Corrosion-Werkstoffe und Korrosion 62(10), pp. 932-942. http://dx.doi.org/10.1002/maco.200905596
[12] Elsener, B., Böhni, H., 1990. Potential Mapping and Corrosion of Steel in Concrete, in “Corrosion Rates of Steel in Concrete, ASTM STP 1065”, Berke, N.S., et al. (Eds.). American Society for Testing and Materials, Philadelphia, pp. 143-156. http://dx.doi.org/10.1520/STP25021S
[13] Matsuoka, K., Kihira, H., Ito, S., Murata, T., 1990: Corrosion Monitoring for Reinforcing Bars in Concrete, in “Corrosion Rates of Steel in Concrete, ASTM STP 1065”, Berke, N.S., et al. (Eds.). American Society for Testing and Materials, Philadelphia, pp. 103-117. http://dx.doi.org/10.1520/STP25018S
[14] John, D. G., Searson, P. C., Dawson, J. L., 1971. Use of AC Impedance Technique in Studies on Steel in Concrete in Immersed Conditions, British Corrosion Journal 16(2), pp. 102-106. http://dx.doi.org/10.1179/000705981798275002
[15] Macdolnad, D. D., Mckubre, M. C. H., Urquidi-Macdonald, M., 1988: Theoretical Assessment of AC Impedance Spectroscopy for Detecting Corrosion of Rebar in Reinforced Concrete, Corrosion 44(1), pp. 2-7. http://dx.doi.org/10.5006/1.3582022
[16] Lemoine, L., Wenger, F., Galland, J., 1990. Study of the Corrosion of Concrete Reinforcement by Electrochemical Impedance Measurement, in “Corrosion Rates of Steel in Concrete, ASTM STP 1065”, Berke, N.S., et al. (Eds.). American Society for Testing and Materials, Philadelphia, pp. 118-133. http://dx.doi.org/10.1520/STP25019S
[17] Scuderi, C. A., Mason, T. O., Jennings, H. M., 1991. Impedance Spectra of Hydrating Cement Pastes, Journal of Material Science 26, pp. 349-353. http://dx.doi.org/10.1007/BF00576526
[18] Song, G., 2000. Equivalent circuit model for AC electrochemical impedance spectroscopy of concrete, Cement and Concrete Research 30, pp. 1723-1730. http://dx.doi.org/10.1016/S0008-8846(00)00400-2
[19] Keddam, M., Takenouti, H., Novoa, X. R., Andrade, C., Alonso, C., 1997. Impedance Measurements on Cement Paste, Cement and Concrete Research 27(8), pp. 1191-1201.http://dx.doi.org/10.1016/S0008-8846(97)00117-8
[20] Dhouibi, L., Triki, E., Raharinaivo, A., 2002. The application of electrochemical impedance spectroscopy to determine the long-term effectiveness of corrosion inhibitors for steel in concrete, Cement & Concrete Composites 24, pp. 35-43. http://dx.doi.org/10.1016/S0958-9465(01)00062-2
[21] Feliu, V., Gonzalez, J. A., Andrade, C., Feliu, S., 1998. Equivalent circuit for modelling the steel-concrete interface. I. Experimental evidence and theoretical prediction, Corrosion Science 40(6), pp. 975-993. http://dx.doi.org/10.1016/S0010-938X(98)00036-5
[22] Ford, S.J., Shane, J.D., Manson, T.O., 1998. Assignment of features in Impedance Spectra of the Cement-Paste/Steel System, Cement Concrete Research 28(12), pp. 1737-1751. http://dx.doi.org/10.1016/S0008-8846(98)00156-2